On the reduction of localization ambiguities of hidden target in the around-the-corner radar

Ba-Huy Pham, Olivier Rabaste, Jonathan Bosse, Israel Hinostroza, Thierry Chonavel

On the reduction of localization ambiguities of hidden target in the around-the-corner radar

Ba-Huy Pham*, Olivier Rabaste*, Jonathan Bosse*, Israel Hinostroza†, Thierry Chonavel§
* DEMR, ONERA, Université Paris-Saclay, F-91123 Palaiseau, France
† SONDRA, CentraleSupelec, Université Paris-Saclay, 91190 Gif-sur-Yvette, France
§ IMT Atlantique, Lab-STICC, UMR CNRS 6285, F-29238, France
Email: *{ba_huy.pham, olivier.rabaste, jonathan.bosse}@onera.fr
†israel.hinostroza@centralesupelec.fr, §thierry.chonavel@imt-atlantique.fr

***Abstract*—Common subspace matched filter in around-the-corner radar exhibits very strong sidelobes that can lead to large localization errors, called here "ambiguities". In this paper, by considering a generalized subspace model which includes the incidental direction measurement, we show that localization performance can be improved significantly. To better observe this improvement, the false localization rate and estimation root-mean-square error performance indices are considered. Localization results highlight the influence of the number of paths to be considered to achieve maximum reduction of localization ambiguities.**

***Index Terms*—around-the-corner radar, multipath exploitation, NLOS, hidden target, ambiguities, urban radar**

I. Introduction

Urban radar applications remains a challenging area of research due to the complexity of the propagation environment induced by the buildings present in the scene. Contrary to conventional radar applications where the target is in radar light-of-sight (LOS), the presence of these buildings generates shadow zones within which a target is not in line of sight and numerous multipaths produced by possible reflections and diffractions on the surrounding surfaces which are often seen as nuisances. Fortunately, these multipaths can be advantageously exploited to detect and locate targets in the shadow zones (or NLOS for Non-Line of Sight). It may then be possible to look behind the corners of walls with a simple hand-held radar: this is called "around-the-corner" radar [1] [2].

There have been several works on this quite recent topic in the past decade. First noticeable works have been conducted in [1] [2] that have shown the feasibility of exploiting multipaths to detect/locate target in NLOS context. More recently, [3] proposed a localization algorithm of NLOS targets by exploiting multipaths time delays and angular measurements. [7] [8] share similar localization approach of NLOS target since they are based on association methods of time of arrivals. [9] [10] proposed a method to locate multiple NLOS targets. The performance of these methods have been proven, but it cannot be achieved without a good knowledge of the scene geometry. Authors of [6] established a propagation model and developed a neural network for NLOS detection and tracking. [11] also used deep neural network in order to classify ghost targets located in LOS.

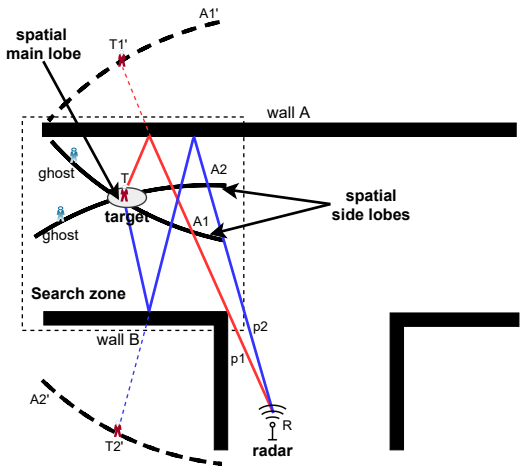

Fig. 1: Illustration of possible localization ambiguities.

Contrary to studies [7] [8] [9] where the target position is deducted from estimated parameters like range or angle of arrival (2-steps localization), we focus here on a 1-step localization approach that directly estimates the target position from the raw signal [14]. The latter approach is often optimal but working in the space of target can induce strong sidelobes, then generates *ambiguities* and makes difficult to accurately locate the target. It is highlighted in [5] that applying subspace matched filter enables to detect and locate a single target behind a corner in 1 step, but the localization results exhibit a large number of ghost positions, as illustrated in Fig. 1. The first reason is that the propagation model, that only takes the round-trip delay measurement into account, assumes that multipath amplitudes are unknown (see III-A). Therefore, any location having at least one multipath delay in common with the true location will have a high detection test level, and then may bias the estimation. In [5], the authors also proposed an algorithm for selecting the optimal number of paths in order to maximize the detection probability, but the impact of the number of paths on the localization ambiguities was not considered. A potential solution was proposed in [4] based on a particle filter in order to benefit from the target dynamic so as to progressively reject ambiguities and improve the

location estimation. The results showed a clear reduction of ambiguities, but this method necessitates several dwell times during the experiment. To our knowledge, the problem of localization ambiguities has not yet been thoroughly studied by the literature.

In this paper, we focus on the mitigation of localization ambiguities of a single target in NLOS by showing that adding incidental direction measurement to the subspace model leads to a clear improvement of localization performance. This improvement is reflected on two metrics: the false localization rate and the root-mean-square error. We also point out that contrary to the [9] [10] the number of multipaths selected in the model may also impact the localization performance, as it does for the detection probability.

The paper is organized as follows. In Section II, the model of radar signal presented in [5] is extended to an array of receiving antennas to enable incidental direction measurement. The origin of localization ambiguities is explained in Section III where we also propose two metrics to evaluate localization performance. Simulation configuration and results are covered in IV. Section V is dedicated to the conclusion.

II. Signal Modelling

Let us assume that a narrow-band signal $s(t)$ is transmitted in the urban scene by a single omni-directionnal antenna. At the reception, we consider a horizontal linear array of Q receiving antennas. Under the far field assumption, the baseband signal received by the q-th elementary antenna is given by

$$r_q(t) = \sum_{m=1}^{M(x,y)} \alpha_m s(t-\tau_m) e^{j\mathbf{k}_{\theta_m}^T \mathbf{x}_q} + n_q(t) \tag{1}$$

where α_m, τ_m and θ_m correspond to the deterministic unknown amplitude, the round-trip time delay and the incidental direction of the m-th path that returns from the single target located at (x, y), respectively. $M(x, y)$ is the number of paths returned by the latter. The term $e^{j\mathbf{k}_{\theta_m}^T \mathbf{x}_q}$ denotes the spatial phase shift induced by multipath m on antenna q, where $\mathbf{k}_{\theta_m} = \frac{2\pi f_0}{c}\mathbf{u}_{\theta_m}$ is the wave vector of m-th path return, f_0 is the carrier frequency, c is the speed of light in the air, $\mathbf{u}_{\theta_m}$ is the unit vector with direction θ_m, and $\mathbf{x}_q$ is the position vector of the q-th antenna. $n_q(t)$ is the additive white noise contribution for the q-th measurement vector, which is assumed to follow a Gaussian circular distribution with known variance σ^2. Note that in Eq. (1) we omit all echoes caused by any fixed obstacles present in the scene such as buildings and trees: we indeed assume that a zero-Doppler rejection processing step has been performed prior to the detection/localization algorithm, by applying for example the method presented in [12], so that all the fixed echoes have been eliminated. After that, the signal in Eq. (1) is sampled with period $T_s \leq 1/B$, where B is the signal bandwidth. Hence we get the following sampled observation vector:

$$\mathbf{r}_q = \begin{bmatrix} r_q(t_1) & r_q(t_2) ... & r_q(t_N) \end{bmatrix}^T, \tag{2}$$

where $t_n = nT_s$. Similarly, we define

$$\mathbf{n}_q = \begin{bmatrix} n_q(t_1) & n_q(t_2) ... & n_q(t_N) \end{bmatrix}^T, \tag{3}$$

$$\mathbf{s}(\tau) = \begin{bmatrix} s(t_1-\tau) & s(t_2-\tau) & ... & s(t_N-\tau) \end{bmatrix}^T. \tag{4}$$

By stacking all received signals $\mathbf{r}_q$ in a single vector $\mathbf{r}$, we define the model of the total received array signal as follows

$$\mathbf{r} = \mathbf{S}(x, y)\boldsymbol{\alpha} + \boldsymbol{n}, \tag{5}$$

where

$$\boldsymbol{\alpha} = \begin{bmatrix} \alpha_1 & \alpha_2 ... & \alpha_{M(x,y)} \end{bmatrix}^T, \tag{6}$$

$$\mathbf{r} = \begin{bmatrix} \mathbf{r}_1^T, \mathbf{r}_2^T, \ldots, \mathbf{r}_Q^T \end{bmatrix}^T, \tag{7}$$

$$\mathbf{n} = \begin{bmatrix} \mathbf{n}_1^T, \mathbf{n}_2^T, \ldots, \mathbf{n}_Q^T \end{bmatrix}^T, \tag{8}$$

$$\mathbf{S} = \begin{bmatrix} \mathbf{S}_1(x,y)^T, \mathbf{S}_2(x,y)^T, \ldots, \mathbf{S}_Q(x,y)^T \end{bmatrix}^T. \tag{9}$$

$\mathbf{S}_q$ is the $N \times M(x, y)$ matrix whose columns are formed by the vectors $\{\boldsymbol{s}_q(\tau_1, \theta_1), \boldsymbol{s}_q(\tau_2, \theta_2), ..., \boldsymbol{s}_q(\tau_{M(x,y)}, \theta_{M(x,y)})\}$ and

$$\boldsymbol{s}_q(\tau, \theta) = \boldsymbol{s}(\tau) e^{j\mathbf{k}_\theta^T \mathbf{x}_q}, \tag{10}$$

where τ and θ depend on (x, y). Note that in the case of a single receiving antenna, Eq. (5) boils down to the model introduced in [5].

A. Subspace Matched Filter (SMF)

The generalized likelihood ratio test (GLRT) and the maximum likelihood estimator for the detection and localization radar problem in Eq. (5) can be derived from using the subspace matched filter [5] [13]. Although the raw signal $\mathbf{r}_q$ contains $M(x, y)$ multipaths, it may be relevant to apply the SMF by considering only a subset of the K strongest paths since it was shown in [5] that there exists an optimal number of paths to select in order to maximize the detection probability. Assuming amplitudes in $\boldsymbol{\alpha}$ are in decreasing order, the SMF is then performed by only taking the first K columns of $\mathbf{S}(x, y)$ in order to form $\mathbf{S}_{1:K}(x, y)$. According to [5], the GLRT is written as

$$T_K(x, y) = \|\mathbf{P}_K(x, y)\boldsymbol{r}\|_2^2 \underset{\mathcal{H}_0}{\overset{\mathcal{H}_1}{\gtrless}} \lambda_K, \tag{11}$$

where $\mathcal{H}_0$ and $\mathcal{H}_1$ correspond classically to the hypothesis of absence and presence of target at location (x, y), respectively. λ_K is the detection threshold set according to the desired false alarm probability (P_{FA}) and $\mathbf{P}$ is the orthogonal projector on the subspace spanned by the columns of $\mathbf{S}_{1:K}(x, y)$:

$$\mathbf{P}_K = \mathbf{S}_{1:K}(x, y)(\mathbf{S}_{1:K}(x, y)^H \mathbf{S}_{1:K}(x, y))^{-1} \mathbf{S}_{1:K}(x, y)^H. \tag{12}$$

The T-level $T_K(x, y)$ also corresponds to the energy of the received signal projected onto the subspace defined by $\mathbf{S}_{1:K}(x, y)$. In case of a single target, the maximum likelihood estimation of the target position is given by

$$(\hat{x}_c, \hat{y}_c) = \underset{(x,y)\in\mathcal{G}}{\arg\max}\, T_K(x, y), \tag{13}$$

where $\mathcal{G}$ is the search zone where the target is located.

III. Localization ambiguities

A. Origin of ambiguities

Ambiguities, as the name suggests, refer to the difficulty in distinguishing the true target position from other positions when applying the SMF algorithm. For instance, in the case of delay-only measurements ($Q = 1$), the SMF provides a high T-level to any position which shares at least a common delay parameter with the true location.

This is mainly due to the SMF statistics in Eq. (12). In this setting, the amplitudes α of the returned multipaths are assumed unknown and are estimated according to the maximum likelihood (ML) criteria. This ML estimator tends to set negligible values to any amplitude α_m that does not correspond to a delay presenting a sufficiently strong energy in the measurement vector. However, several locations share some (at least one) common delays with the target position. When projecting the received signal onto the subspace of such an ambiguous location, common paths are estimated with high amplitudes whereas different ones are omitted. Then false positions have relatively high T-level even if they do not share all common measurements with the true position. This phenomenon is very similar to the presence of sidelobes in classical radar leading to poor parameter estimation, although ambiguities are much stronger in the around-the-corner radar.

Such ambiguities arise in various situations. The first simpler one is illustrated geometrically in Fig. 1, where ghost positions are distributed on equirange circle arcs from the radar for a given multipath distance corresponding to the target position. These ambiguities are provided by paths that share similar reflections with the true position. Their inherently high T-level may surpass that of the true position (in presence of noise) with a non negligible probability, then resulting in false localization.

More generally, ambiguities can arise with positions whose paths do not share the same reflection surface as the true position, but still present a similar time delay. Thus it is generally difficult to determine the form of the localization ambiguities, especially in a complex scene geometry. Therefore, in the next section we introduce two metrics in order to quantify the ambiguity problem.

B. Ambiguity metrics

In order to measure the impact of ambiguities on the localization performance of the SMF with or without the additional angular measurement, we define the neighbourhood of the true target position (x_c, y_c) as the set of unresolved locations around the true position. Since the SMF algorithm is classically applied on a grid of positions, then an appropriate grid step has to be found. Its choice is more involved than for the classical radar in LOS problem because the radar resolution (-3 dB main lobe width) and depends on the true target position. We choose a simple grid step which is proportional to the radar range resolution.

Concretely, for a given grid $\mathcal{G}$, we define the target vicinity as

$$\mathcal{C}(x_c, y_c) = \left\{ (x, y) \in \mathcal{G}, \sqrt{(x - x_c)^2 + (y - y_c)^2} \leq \frac{c}{2B} \right\} \tag{14}$$

Therefore localization of the target at position (x_c, y_c) is said *ambiguous* if

$$\max_{(x,y) \notin \mathcal{C}(x_c, y_c)} T_K(x, y) > T_K(x_c, y_c) > \lambda_K \tag{15}$$

We define then the *false localization rate* (FLR) at (x_c, y_c), noted $\text{FLR}(x_c, y_c)$ as the rate to which condition (15) occurs. In other words, it explains how frequently a position beyond the target vicinity is detected and maximizes the T-level in presence of noise. Furthermore, we also consider the RMSE metric for position estimation

$$\text{RMSE}(x_c, y_c) = \sqrt{\mathbb{E}[(\hat{x}_c - x_c)^2 + (\hat{y}_c - y_c)^2]}. \tag{16}$$

$\text{RMSE}(x_c, y_c)$ denotes the *root-mean-square error* in localization at (x_c, y_c). Finding the analytic expressions of both preceding metrics is not obvious, but their value can be estimated numerically via Monte Carlo simulation.

C. Influence of the number of selected paths

According to [5], the analytical expression of the detection probability (P_D) depends both on the signal-to-noise ratio (SNR) and λ_K. More specifically, P_D increases with the SNR, defined as

$$\text{SNR} = \frac{\|\mathbf{S}_{1:K}(x, y)\boldsymbol{\alpha}\|_2^2}{\sigma^2}, \tag{17}$$

(i.e P_D increases when K grows), but decreases with respect to λ_K which is a decreasing function of K.

Consequently, adding more paths to the model may help to improve the detection probability, but the energy of each added path has to be sufficiently strong to compensate the corresponding increase of the detection threshold. Therefore, an optimal value of K can be found in terms of maximizing P_D [5].

A natural question arises then: do we observe a similar phenomenon for the localization ambiguities? Indeed, since the FLR and RMSE criteria depend on the SMF output $T_K(x, y)$ whose statistical distribution depends on $\mathbf{S}_{1:K}(x, y)$, the number of paths may be chosen in order to minimize both metrics. Hence, in the following sections, we show by simulations that the number of considered paths indeed has an impact on the localization performance, and a trade-off between detection and localization criteria should be found.

IV. Numerical results

A. Configuration

The localization performance is evaluated by simulations. To do this, a 10 GHz FMCW radar system is considered, that consists of a linear array with Q receiving antennas with half wavelength spacing. The transmitted waveform bandwidth is $B = 300$ MHz, and thus the range resolution is 0.5 m. Simulations are performed for two configurations: a single receiving

antenna ($Q = 1$) and 10 receiving antennas ($Q = 10$). The first configuration corresponds to the case where only the time delay measurements are used (as in [5]) whereas the second contains both delay and incidental direction information.

The simulation scenario is a typical urban T-junction as shown in Fig. 2. In the region of interest, the radar and the NLOS target local coordinates are $(0, 2)$ and $(35.60, 14.87)$ meters, respectively. As in [5], the search zone is divided into cells of the same size of 0.25×0.25 m, that corresponds roughly to half the radar range resolution. For each point (x, y) on this grid, a ray tracing simulation is performed in order to determine the multipaths associated to the corresponding position with their respective time delays and incidental direction parameters, thus enables building of the matrix $\mathbf{S}(x, y)$. The received signal $\mathbf{r}$ is generated by using the multipaths generated for the target position, and adding propagation losses proportional to $1/D^2$, where D is the propagation distance, as well as reflection losses of -8 dB for each reflection. For a fair comparison, the same received SNR is set in both aforementioned configurations, which means that in the case of $Q = 10$, the target radar cross section is set to be 10 times smaller than that of $Q = 1$.

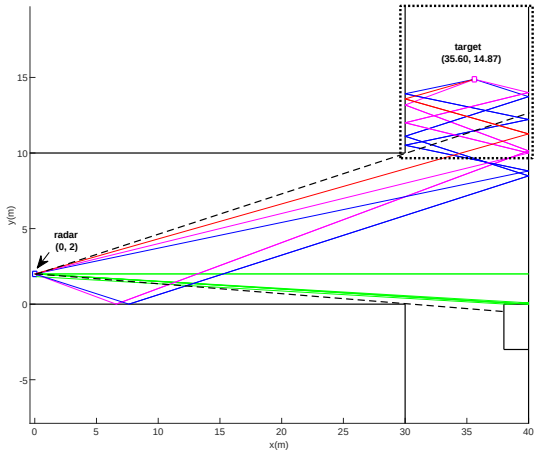

Fig. 2: T-junction urban scenario. The search zone is enclosed by the dotted line. The target is located in a NLOS zone above the dashed line

B. Localization results

Fig. 3 shows the localization map for the two configurations in a noiseless case with $K = 5$ paths used in the SMF test. These maps correspond to the ambiguity figures for the considered scenario. In both cases, the true position presents the highest T-level (about 0 dB). For $Q = 1$ (Fig. 3a), the ambiguity figure exhibits circle arcs of high T-level positions whereas for $Q = 10$ (Fig. 3b), these circle arcs are significantly attenuated. This improvement is due to the contribution of the incidental direction information that lowers the signal energy contained in ghost positions subspace. Since this improvement is equivalent to reducing the sidelobes in classical radar, it is expected that in presence of noise, the probability that ghost

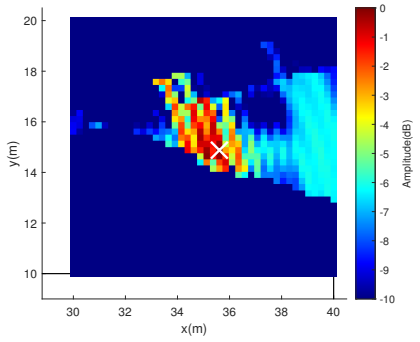

(a) Q = 1

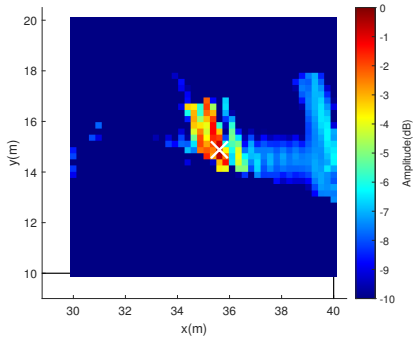

(b) Q = 10

Fig. 3: Localization maps for a target located in NLOS. The target position $(35.60, 14.87)$ is marked by the white cross. (a) one single antenna (b) 10 receiving antennas.

positions are detected and surpass the true target position T-level will be reduced in case of multi-receiving antennas comparing to the single antenna configuration.

Fig. 4 shows the resulting estimated FLR and RMSE for the considered scenario. At first glance, a significant gap can be observed between the performance provided by the single antenna and the array with 10 antennas. Fig. 4a shows that when $Q = 10$, the FLR value decreases more rapidly than when $Q = 1$, and has a smaller RMSE which tends rapidly towards 0 at high SNRs, as shown in Fig. 4b. Interestingly, FLR curves tendency is related to the detection probability curve: at low SNRs, the FLR is insignificant since the true target position and the ghost ones are not detected. At medium SNRs, although higher T-level at the true target position enables to detect it more frequently, it is not strong enough to compete with the raise of T-level at ghost positions, then results in high FLR. At high SNRs, the maximal of T-level corresponds to the target position and it is completely detected with high probability, as seen in Fig. 3, then the FLR decreases.

Fig. 5 represents the FLR and RMSE with respect to the number of paths K used for the SMF and for an SNR of 20 dB. It appears that the localization performance depends upon the number of paths considered. For $Q = 1$, FLR and RMSE are highest when $K = 1$. By adding other paths, the values of FLR and RMSE decrease until the optimal point $K = 3$. Then, if K keeps growing, the curves of FLR and RMSE rise again. It can be explained by the fact that the

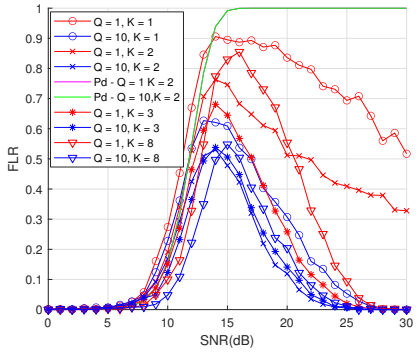

(a) FLR

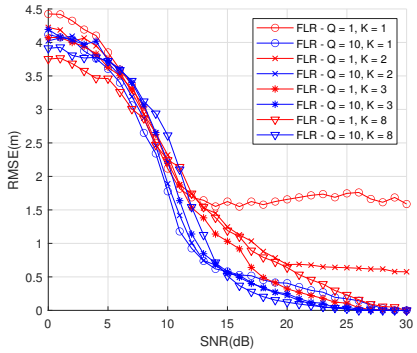

(b) RMSE

Fig. 4: Estimated FLR and RMSE for a target located at $(35.60, 14.87)$ for different SNRs and numbers of considered paths for the model K. $P_{FA} = 10^{-6}$, 1000 Monte Carlo runs.

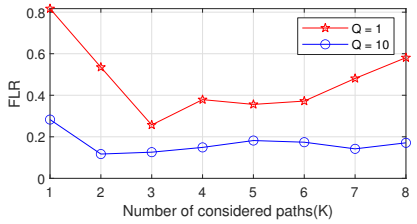

(a) FLR

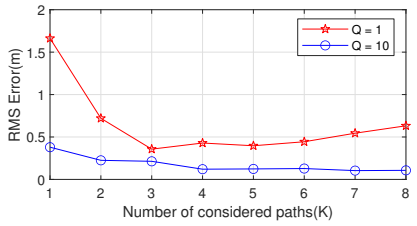

(b) RMSE

Fig. 5: FLR and RMSE as a function of number of considered paths K in the model. SNR = 20 dB, 1000 Monte Carlo runs.

information provided by additional paths contribute to mitigate ambiguities, but the more we add new paths the more new ghost positions appear, then the localization performance will deteriorate. Thus, it seems that there is an optimal number of paths to be considered in terms of localization performance. This tendency is less sensitive for $Q = 10$ thanks to incidental direction information that strongly reduces ghost positions.

V. Conclusion

In this paper, we have studied the impact of angle of arrival information conveyed by array antenna observation on the reduction of localization ambiguities of a single NLOS target in around-the-corner radar. Simulation results show that the multi-receiving antenna configuration yields better localization performance than the single receiving antenna case as considered in [5], with lower rate of false localization (FLR) and estimation bias (RMSE). Moreover, it seems that there can be an optimal number of significant paths to be selected for the model in order to minimize the false localization rate, that may compromise the number of paths selection criterion in terms of maximizing detection probability proposed in [5].

References

[1] A. Sume et al., "Radar Detection of Moving Targets Behind Corners," in IEEE Transactions on Geoscience and Remote Sensing, vol. 49, no. 6, pp. 2259-2267, 2011.

[2] P. Setlur, G. E. Smith, F. Ahmad and M. G. Amin, "Target Localization with a Single Sensor via Multipath Exploitation," in IEEE Transactions on Aerospace and Electronic Systems, vol. 48, no. 3, pp. 1996-2014, 2012.

[3] Q. Zhao, G. Cui, S. Guo, W. Yi, L. Kong and X. Yang, "Millimeter Wave Radar Detection of Moving Targets Behind a Corner," 2018 21st International Conference on Information Fusion (FUSION), pp. 2042-2046, 2018.

[4] K. Thai, O. Rabaste, J. Bosse and T. Chonavel, "GLRT Particle Filter for Tracking Nlos Target in Around-the-Corner Radar," 2018 IEEE International Conference on Acoustics, Speech and Signal Processing (ICASSP), pp. 3216-3220, 2018.

[5] K. Thai, O. Rabaste, J. Bosse, D. Poullin, I. H. Sáenz, T. Letertre, T. Chonavel, "Detection–Localization Algorithms in the Around-the-Corner Radar Problem," in IEEE Transactions on Aerospace and Electronic Systems, vol. 55, no. 6, pp. 2658-2673, 2019.

[6] N. Scheiner, F. Kraus, F. Wei, B. Phan, F. Mannan, N. Appenrodt, et al, "Seeing Around Street Corners: non-line-of-sight detection and tracking in-the-wild using doppler radar," in proc. IEEE Conf. Comput. Vis. Pattern Recog., Los Angeles, CA, USA, 2019.

[7] Huagui Du, Chongyi Fan, Zhen Chen, Chun Cao, and Xiaotao Huang, "NLOS Target Localization with an L-Band UWB Radar via Grid Matching," Progress In Electromagnetics Research M, Vol. 97, 45-56, 2020.

[8] S. Fan, Y. Wang, G. Cui, S. Li, S. Guo, M. Wang, L. Kong, "Moving Target Localization Behind L-shaped Corner With a UWB Radar," 2019 IEEE Radar Conference (RadarConf), 2019, pp. 1-5, doi: 10.1109/RADAR.2019.8835790.

[9] S. Guo, S. Li, G. Cui, S. Fan, L. Kong and X. Yang, "MIMO Radar Localization of Targets Behind L-shaped Corners," 2020 IEEE 11th Sensor Array and Multichannel Signal Processing Workshop (SAM), pp. 1-4, 2020.

[10] S. Li, S. Guo, J. Chen, X. Yang, S. Fan, C. Jia, G. Cui, H. Yang, "Multiple Targets Localization Behind L-Shaped Corner via UWB Radar," in IEEE Transactions on Vehicular Technology, vol. 70, no. 4, pp. 3087-3100, 2021.

[11] M. Chamseddine, J. Rambach, D. Stricker and O. Wasenmuller, "Ghost Target Detection in 3D Radar Data using Point Cloud based Deep Neural Network," 2020 25th International Conference on Pattern Recognition (ICPR), pp. 10398-10403, 2021.

[12] F. Colone, D. W. O'Hagan, P. Lombardo and C. J. Baker, "A Multistage Processing Algorithm for Disturbance Removal and Target Detection in Passive Bistatic Radar," in IEEE Transactions on Aerospace and Electronic Systems, vol. 45, no. 2, pp. 698-722, 2009

[13] L. L. Scharf and B. Friedlander, "Matched subspace detectors," in IEEE Transactions on Signal Processing, vol. 42, no. 8, pp. 2146-2157, 1994.

[14] A. J. Weiss, "Direct Geolocation of Wideband Emitters Based on Delay and Doppler," in IEEE Transactions on Signal Processing, vol. 59, no. 6, pp. 2513-2521, 2011.